X-ray photoelectron spectroscopic study of $Ge_2Sb_2Te_5$ etched by fluorocarbon inductively coupled plasmas

S.-K. Kang,[1] J. S. Oh,[2] B. J. Park,[2] S. W. Kim,[2] J. T. Lim,[2] G. Y. Yeom,[1,2,a)] C. J. Kang,[3] and G. J. Min[3]

[1]*SKKU Advanced Institute of Nanotechnology, Sungkyunkwan University, Suwon, Gyeonggi-do 440-746, Republic of Korea*

[2]*Department of Advanced Materials Science and Engineering, Sungkyunkwan University, Suwon, Gyeonggi-do 440-746, Republic of Korea*

[3]*Memory Division, Samsung Electronics Co. Ltd., Yongin City, Gyeonggi-do 440-746, Republic of Korea*

(Received 13 March 2008; accepted 14 July 2008; published online 1 August 2008)

X-ray photoelectron spectroscopy was used to determine the level of surface fluorination damage of $Ge_2Sb_2Te_5$ (GST) etched by fluorocarbon gases at different F/C ratios. When blank GST was etched, the gas with a higher F/C ratio produced a thinner C–F polymer on the etched surface but fluorinated Ge, Sb, and Te compounds were observed in the remaining GST. When the sidewall of the etched GST features was investigated, a thicker fluorinated layer was observed on the GST sidewall etched by the higher F/C ratio gas, indicating more fluorination due to the difficulty in preventing F diffusion into the GST through the thinner C–F layer. © *2008 American Institute of Physics*. [DOI: 10.1063/1.2967468]

Recently, phase-change random access memory (PRAM) has made prominent progress in memory performance and has brought a bright prospect for the next generation nonvolatile memory (NVM) technologies in companies with its competitive candidates such as ferroelectric random access memory and magnetoresistive random access memory.[1–3] Among them, PRAM is a rapidly emerging candidate for the next generation NVM due to its excellent advantages such as high-speed, high-density, low power consumption, nonvolatility, and competitive cost. One of the chalcogenide-based phase-change materials that has been observed for nanoscale nonvolatile memories is the $Ge_2Sb_2Te_5$ (GST) ternary alloy[4] even though the understanding of the chemical state and etch characteristics of GST is incomplete.

For the operation of GST, a stoichiometric composition needs to be maintained for high-speed phase-change transformations and a high degree of cyclability. Also, during the etching of GST, the composition needs to be maintained with no degradation. However, it is known that the GST material is easily damaged during etching by halogen-gas-based plasmas, and it is difficult to maintain its sidewall composition without halogenation-induced degradation.

In this article, the degree of surface degradation of GST during etching by fluorocarbon plasmas with different F/C ratios was investigated by x-ray photoelectron spectroscopy (XPS) to study the possibility of preventing the sidewall degradation by the formation of a C–F layer on the sidewall of etched GST.

As samples, 100 nm thick GST thin films were prepared on SiO_2/Si substrates by rf magnetron cosputtering from GeTe and Sb_2Te_3 targets. Some of the samples were patterned with a SiO_2 hard mask after depositing the Ti/TiN layer on the GST films by dc magnetron sputtering without breaking the vacuum. The etching experiments for the GST films were performed in an 8 in. diameter inductive coupled plasma (ICP) etching system (STS PLC, UK) operated at a frequency of 13.56 MHz. The etch depth variations were measured using a surface profiler (Alpha-Step 500, Tencor), and the etch profiles of the patterned GST samples were examined by a field emission scanning electron microscopy (SEM) (Hitachi S-4700). The chemical bonding characteristics of the GST films after etching were examined by the XPS (ESCA2000, VG Microtech Inc.) using an Al $K\alpha$ twin anode source with a photon energy of 1486.6 eV.

Figure 1 shows the etch rate of GST and C 1*s* spectra measured by XPS from the surface of the partially etched bare GST films as a function of the F/C ratio using CF_4, 50% CF_4/50% C_4F_8, and C_4F_8 while maintaining a flow rate and operating pressure of 100 SCCM (SCCM denotes cubic centimeter per minute at STP) and 7 mTorr, respectively. The rf inductive power and bias voltage were maintained at 500 W and −150 V, respectively. As shown in the figure, C 1*s* peak

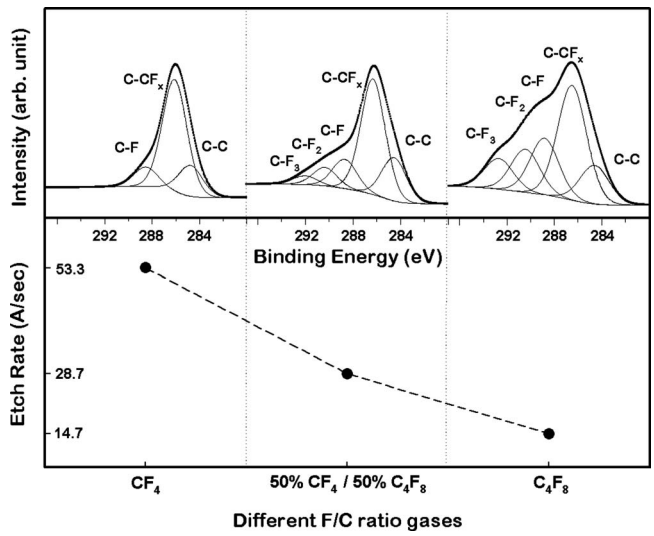

FIG. 1. GST etch rate (Å/s) in the ICP etching system and C 1*s* XPS spectra of the GST surface partially etched in fluorocarbon plasmas with different F/C ratios.

a)Author to whom correspondence should be addressed. Tel.: +82 31 299 6560. FAX: +82 31 299 6565. Electronic mail: gyyeom@skku.edu.

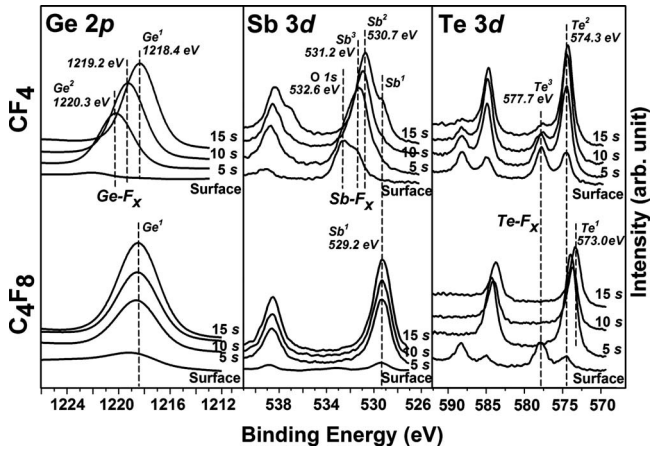

FIG. 2. XPS spectra of each component of the GST films after the etching in CF_4 and C_4F_8 plasmas as a function of the sputter time during Ar^+ ion depth profiling.

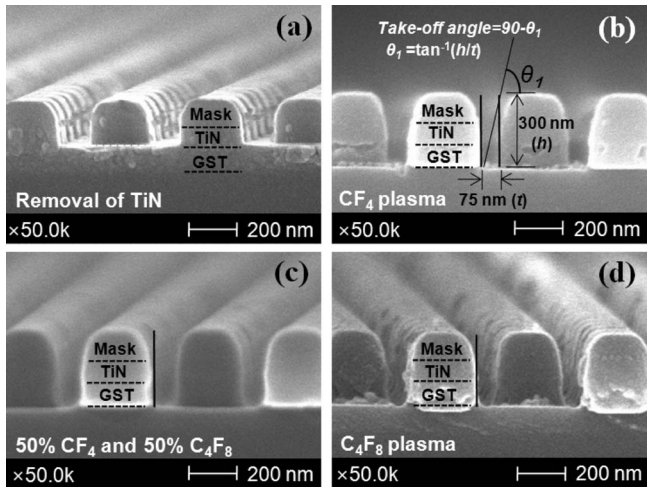

FIG. 3. Cross-sectional SEM images of the patterned GST samples for etch steps. (a) The GST pattern after removing the Ti/TiN layer [process condition: 5 mTorr of BCl_3 (15 SCCM)/Cl_2 (15 SCCM)/Ar (70 SCCM), 1 kW of inductive power, −75 V of dc bias voltage, and 20 s of etch time]. (b) GST etched by CF_4 plasma, (c) GST etched by 50% CF_4/50% C_4F_8 plasma, and (d) GST etched by C_4F_8 plasma. (Process condition for GST etching: 7 mTorr, 100 SCCM, 500 W of inductive power, and −150 V of dc bias voltage).

measured on the GST showed different binding states for the different F/C ratios such as C–C at 284.5 eV, C−CF_x at 286.3 eV, and C−F_x (x=1,2,3) at 288.7, 290.2, and 292.5 eV, respectively. The decrease in the F/C ratio increased not only the total binding peak intensity but also the relative intensities of the C−F_x binding peaks compared to the C−CF_x binding peak. Therefore, at a lower F/C gas ratio, a thicker and more Teflon-like layer was formed on the GST surface during the etching as reported elsewhere.[5–8] The decrease in the GST etch rate with the etching gas with a lower F/C ratio, as shown in the figure, is also related to the formation of the C–F polymer layer on the GST surface during etching, which prevents direct reactions such as diffusion of fluorine radicals and energetic F^+ ions into the GST films.[9]

The differences in the polymer layer formed on the GST surface during etching also varied in the depth at which the fluorinated compound had formed in the GST layer. Figure 2 shows the XPS binding peak spectra of Ge, Sb, and Te after Ar^+ ion depth profiling of the blank GST films etched by CF_4 and C_4F_8 under the process conditions shown in Fig. 1. The ion-gun energy and ion current were set to 3 kV and 2 μA, respectively. For Ge 2p, the binding peaks were observed at 1218.4 (Ge^1) and 1220.3 eV (Ge^2), originating from Ge–Te and Ge−F_x, respectively, as observed by previous researchers.[10,11] The peak at 1219.2 eV observed after etching for 10 s appears to be a mixture of Ge^1 and Ge^2. In the case of Sb $3d_{5/2}$, the binding peaks were observed at 531.2 (Sb^3), 530.7 (Sb^2), and 529.2 eV (Sb^1). Among these peaks, Sb^1 is from the metallic homopolar bonding between Sb and Te. Sb^3 and Sb^2 are believed to originate from Sb−F_x, while another binding energy peak observed at 532.6 eV appears to be related to the oxygen bonding formed on the surface during air exposure prior to XPS analysis. For the spectra of Te $3d_{5/2}$, the peaks are observed at 577.7 (Te^3), 574.3 (Te^2), and 573.0 eV (Te^1), where Te^1 and Te^2 originated from the metallic peak related to Te–Te and Ge–Te (or Sb–Te), respectively, and Te^3 is believed to be from Te−F_x.

After etching, the GST surface appeared to be Ge deficient and covered with a fluorocarbon layer. After 5 s sputtering with Ar^+ ions, the fluorocarbon layer on the surface was removed effectively by revealing each component of GST. When the peak intensities of Ge 2p, Sb $3d_{5/2}$, and Te $3d_{5/2}$ peaks on the GST surfaces etched with CF_4 and C_4F_8 were compared, the GST surface etched with C_4F_8 showed the binding energy peaks related to the metallic bonds, indicating no fluorination of the component even after 5 s sputtering. However, in the case of the GST surface etched by CF_4, the surface showed a shift in the binding energy corresponding to Ge−F_x, Sb−F_x, and Te−F_x of up to 15 s sputtering. Therefore, deeper fluorine penetration was observed in the GST etched by CF_4.

In addition to the degradation of the GST surface during etching with the fluorocarbon gases, the sidewall degradation of the GST features during etching of the patterned GST was investigated. Figure 3 shows SEM images of the patterned and etched GSTs. The stacked GST patterns were prepared with a SiO_2-mask/Ti (as an adhesion layer at 5 nm)/TiN (as a diffusion barrier and mask for the GST layer)/GST/SiO_2 stacks. A two-step etch process was applied in this experiment. In the first step, the Ti/TiN layer was removed under the following conditions: 5 mTorr of BCl_3 (15 SCCM)/Cl_2 (15 SCCM)/Ar (70 SCCM), 1 kW of inductive power, −75 V of dc bias voltage, and 20 s of etch time. After this step, the surface corresponded to the nonrecess of the GST layer. Figure 3(a) shows this feature. In the second step, the etching of GST was performed with 100 SCCM of either CF_4, 50% CF_4/50% C_4F_8, or C_4F_8 at 500 W inductive source power and dc bias voltage of −150 V for 20–70 s. The etched features are shown in Figs. 3(b)–3(d) for the etching by CF_4, 50% CF_4/50% C_4F_8, and C_4F_8, respectively. As shown in the figures, an almost vertical etching of the GST layer was obtained. The XPS analysis was performed at a tilted angle to examine the sidewall of the GST etched with fluorocarbon plasmas.

Figure 4 shows the XPS spectra of each component of the etched GST sidewalls. In order to irradiate x rays onto the whole sidewall surface, as represented in Fig. 3(b), the samples were tilted by 14°. In the case of Sb $3d_{5/2}$, due to the overlap between the O 1s peak from the SiO_2 hard mask remaining on the GST features and the fluorinated Sb $3d_{5/2}$ peak, smaller binding peaks observed for Sb $3d_{3/2}$ at 539.3

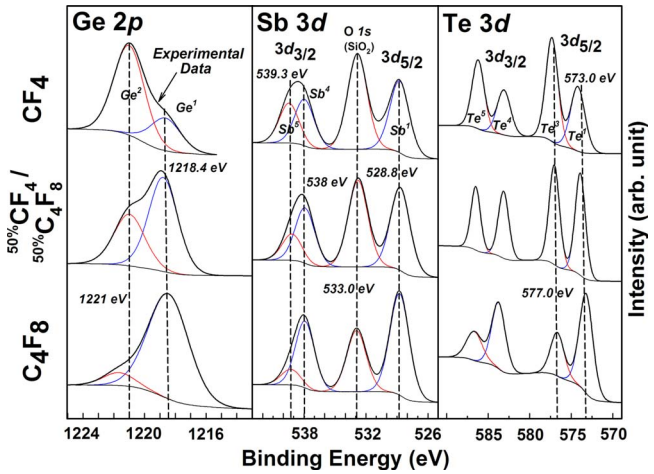

FIG. 4. (Color online) Angular XPS spectra of Ge, Sb, and Te in the patterned GST sidewall etched with fluorocarbon gases at different F/C ratios.

eV (Sb^5: fluorinated Sb) and 538 eV (Sb^4: metallic Sb) were used for the analysis by knowing that the peak intensity ratio of $3d_{3/2}$:$3d_{5/2}$ (Sb^4:Sb^1) is 2:3. As shown in this figure, the XPS spectra of each component for the etched GST sidewalls showed both fluorinated peaks at approximately 1221 (Ge^2), 539.3 (Sb^5), and 577 eV (Te^3) and metallic peaks at approximately 1218.4 (Ge^1), 538 (Sb^4), and 573 eV (Te^1), possibly due to the thin fluorinated layer formed on the sidewall during etching. When intensity ratios were considered, the intensity ratios of $Ge^2/(Ge^1+Ge^2)$ for the Ge $2p$ spectra after etching in CF_4, 50% CF_4, /50% C_4F_8, and C_4F_8 were 0.74, 0.37, and 0.09, respectively. The intensity ratios of $Sb^5/(Sb^4+Sb^5)$ for the Sb $3d_{3/2}$ spectra were 0.46, 0.32, and 0.19 for those gases; and those of $Te^3/(Te^1+Te^3)$ for the Te $3d_{5/2}$ spectra were 0.58, 0.50, and 0.31. Therefore, the increase in the F/C ratio increased the fluorinated peak intensity compared to the metallic peak intensity. A decrease in the F/C ratio in the etching gas resulted in the formation of a thicker and Teflon-like C–F polymer film on the GST sidewall (not shown), similar to the blank etched GST shown in Fig. 1. Hence, the degree of fluorination of the etched GST sidewall is related to the thickness and composition of the C–F polymer formed on the sidewall of the etched GST, which protects the sidewall from fluorination during etching by fluorocarbon gases.

In summary, blank and patterned GST samples were etched by fluorocarbon gases with different F/C ratios and the degree of surface fluorination was examined by XPS. The use of a fluorocarbon gas with a lower F/C ratio resulted in a lower GST etch rate due to the thicker C–F polymer formed on the GST surface during etching. However, the formation of the thicker C–F polymer decreased fluorination of the exposed GST surface and sidewalls offering protection against the diffusion of fluorine radicals and F^+ ions during etching. It is believed that, by using fluorocarbon gas composed of a low F/C ratio, the surface and sidewall degradation by fluorination during etching can be effectively protected.

This study was supported by Samsung Electronics and the National Program for Tera-Level Nanodevices of the Korean Ministry of Education, Science and Technology (MEST) as a 21st Century Frontier Program.

[1] M. H. R. Lankhorst, B. W. S. M. M. Ketelaars, and R. A. M. Wolters, Nat. Mater. **4**, 347 (2005).
[2] S. Lai and T. Lowery, Proceedings of the IEEE International Electron Devices Meeting, 2001 (unpublished), Vol. 36, p. 5.1.
[3] K. Nakayama, K. Kojima, Y. Imai, T. Kasai, S. Fukushima, A. Kitagawa, M. Kakimoto, Y. Kakimoto, and M. Suzuki, Jpn. J. Appl. Phys., Part 1 **42**, 404 (2003).
[4] N. Yamada, E. Ohno, K. Nishiuchi, and N. Akahira, J. Appl. Phys. **69**, 2849 (1991).
[5] D. Zhang and M. J. Kushner, J. Vac. Sci. Technol. A **19**, 524 (2001).
[6] K. Takahashi, M. Hori, S. Kishimoto, and T. Goto, Jpn. J. Appl. Phys., Part 1 **33**, 4181 (1994).
[7] F. H. Bell, O. Joubert, G. S. Oehrlein, Y. Zhang, and D. Vender, J. Vac. Sci. Technol. A **12**, 3095 (1994).
[8] L. Rolland, M. C. Peignon, Ch. Cardinaud, and G. Turban, Microelectron. Eng. **53**, 375 (2000).
[9] T. E. F. M. Standaert, C. Hedlund, E. A. Joseph, and G. S. Oehrlein, J. Vac. Sci. Technol. A **22**, 53 (2004).
[10] A. Thompson, I. Lindau, D. Attwood, P. Pianetta, E. Gullikson, A. Robinson, M. Howells, J. Scofield, K.-J. Kim, J. Underwood, J. Kirz, D. Vaughan, J. Kortright, G. Williams, and H. Winick, *X-Ray Data Booklet*, 2nd ed. (Lawrence Berkeley National Laboratory, Berkeley, CA, 2001).
[11] J. F. Moulder, W. F. Stickle, P. E. Sobol, and K. D. Bomben, *Handbook of X-Ray Photoelectron Spectroscopy* (Perkin-Elmer, Eden Prairie, MN, 1992).